AGU PUBLICATIONS

JGR

Journal of Geophysical Research: Atmospheres

RESEARCH ARTICLE
10.1002/2016JD025073

Key Points:
- Compared to CERES, MISR is darkening and MODIS is brightening, by ~1% per decade
- The dependence of the spectral to broadband radiance ratio on precipitable water content is minimized by use of Dome C
- The intercalibration of CERES and MISR successfully corrects the differential TOA albedo trends at low and middle latitudes

Correspondence to:
R. Davies,
r.davies@auckland.ac.nz

Citation:
Zhan, Y., and R. Davies (2016), Intercalibration of CERES, MODIS, and MISR reflected solar radiation and its application to albedo trends, *J. Geophys. Res. Atmos.*, *121*, 6273–6283, doi:10.1002/2016JD025073.

Received 10 MAR 2016
Accepted 29 MAY 2016
Accepted article online 2 JUN 2016
Published online 11 JUN 2016

Intercalibration of CERES, MODIS, and MISR reflected solar radiation and its application to albedo trends

Yizhe Zhan[1] and Roger Davies[1]

[1]Department of Physics, University of Auckland, Auckland, New Zealand

Abstract Measurements on the Terra satellite by the Cloud and the Earth's Radiant Energy System (CERES), the Moderate Resolution Imaging Spectroradiometer (MODIS), and the Multiangle Imaging Spectroradiometer (MISR), between 2001 and 2015 over the polar regions, are analyzed in order to investigate the intercalibration differences between these instruments. Direct comparisons of colocated near-nadir radiances from CERES, MODIS, and MISR show relative agreement within 2.4% decade^{-1}. By comparison with the CERES shortwave broadband, MODIS Collection 6 is getting brighter, by $1.0 \pm 0.7\%$ decade^{-1} in the red band and $1.4 \pm 0.7\%$ decade^{-1} in the near infrared. MISR's red and near-infrared bands, however, show darkening trends of $-1.0 \pm 0.6\%$ decade^{-1} and $-1.1 \pm 0.6\%$ decade^{-1}, respectively. The CERES/MODIS or CERES/MISR visible and near IR radiance ratio is shown to have a significant negative correlation with precipitable water content over the Antarctic Plateau. The intercalibration results successfully correct the differential top-of-atmosphere trends in zonal albedos between CERES and MISR.

1. Introduction

Satellite-based measurements of radiant fluxes scattered or emitted by the Earth are crucial to the understanding of climate and to monitoring changes in climate. The ability to detect change, however, is severely limited by the short duration and the calibration uncertainty of individual satellite radiometers. With the continued success of the Multiangle Imaging Spectroradiometer (MISR), Moderate Resolution Imaging Spectroradiometer (MODIS), and Cloud and the Earth's Radiant Energy System (CERES) instruments on the Terra satellite, launched in December 1999, we can exploit the intercomparison of radiances measured simultaneously by these three instruments to maximize the information content of Terra regarding changes. In the following, we examine the intercalibration differences between MISR, MODIS, and CERES and show how the combined intercalibration improves the precision that is attainable separately.

In earlier work, *Loeb et al*. [2007] found that the radiances measured by CERES, MODIS, and MISR remained stable relative to one another to better than 1% from 2000 to 2005. *Wu et al*. [2014], however, noted calibration differences between MISR and MODIS of up to 4% between 2000 and 2014, particularly for red and near-infrared (NIR) radiances. The availability of the longer time series prompts us to investigate the differences between the three instruments and to further refine their intercalibration at the radiance level in order to improve long-term trend detection [*Weatherhead et al*., 1998]. As noted by *Wielicki et al*. [1996], there are two aspects that affect the long-term trend detection: spatial sampling noise (random with no trend) and long-term instrument drift. Here we reduce the sampling noise by considering monthly means for April and October, for two relatively large (2°latitude by 3°longitude) uniform polar areas.

We consider near-simultaneous colocated radiances measured by MODIS, MISR, and CERES from 2001 to 2015. We apply a normalized ratio method to examine the relative calibration differences between the three instruments. Five sets of comparison for two regions are discussed. The role of low water vapor content in the broad-to-narrow radiance relationship is also considered. Having obtained a fresh intercalibration of MODIS, MISR, and CERES on Terra, we apply this result to the analysis of high-latitude albedo trends, especially evident for Arctic regions.

2. CERES, MODIS, and MISR Instrument Calibration

Here we summarize the individual calibration procedures for the CERES, MODIS, and MISR instruments. These have been well maintained throughout the Terra mission using independent onboard calibrator (OBC) procedures [*Matthews et al*., 2005; *Bruegge et al*., 2007; *Sun et al*., 2012].

CERES carries out biweekly solar and internal checks on the sensor responses [*Lee et al*., 1996; *Wielicki et al*., 1996]. The resulting gains and offsets are then verified by validation studies and revised only if the sensor responses degrade by more than 1% in the shortwave region. By analyzing CERES observations from 2000 to 2004, *Matthews et al*. [2005] found there was an unexplainable drop of up to 2% in the shortwave flux. They attributed this drop to spectral darkening in the blue ultraviolet spectral region caused by contamination of the optics. A scene-specific adjustment was then made to all measurements, leading to the release of the Edition 3A data set. They claimed a stability target of 0.3% per decade is achievable in the new release [*Matthews et al*., 2005]. More recently, *Daniels et al*. [2015] suggested an even smaller change of 0.15% per decade for CERES FM1 shortwave band can be achieved by analyzing the lunar observations.

In our study, we use the current version of CERES Single Satellite Footprint (SSF) top-of-atmosphere (TOA)/Surface Fluxes and Clouds (CERES_Terra_FM1_Edition_3A_SSF) data set, since CERES Flight Model One (FM1) is used as the standard instrument to correct the radiometric scale for FM1 and FM2 on board Terra. The SSF product combines the broadband CERES radiation with imager-based cloud and aerosol properties from MODIS measurements. CERES SSF Edition 3A uses MODIS collection 4 as inputs before 30 June 2006, after which it uses collection 5.

The reflective solar bands (RSB) of MODIS consist of bands 1–19 and 26 with spectral range from 0.412 μm to 2.13 μm. These are calibrated by the combination of a Solar Diffuser (SD), a Solar Diffuser Stability Monitor (SDSM), and a Spectroradiometric Calibration Assembly (SRCA). The SD is used to establish the RSB calibration of the reflectance factor product, and the corresponding radiances are then derived from a solar spectral irradiance model [*Guenther et al*., 2002]. During the SD calibration period, the SDSM alternately measures light reflected off the SD and direct solar irradiance to track potential changes in SD reflectance. The SRCA provides limited utility for MODIS radiometric observations and is mainly used to assess the stability of the spectral and pixel positions.

The degradation of the MODIS response is wavelength, mirror-side, and angle-of-incidence (AOI) dependent [*Guenther et al*., 2002; *Xiong et al*., 2002], and thought to be caused by thin film depositions on optics followed by solarization of that film through ultraviolet exposure [*Guenther et al*., 2002]. The degradation of the MODIS SD, however, is wavelength dependent [*Xiong et al*., 2002]. Based on the first year of MODIS data, *Guenther et al*. [2002] showed there were 0.2% and 0.5% SD degradation for MODIS bands 1 and 2, respectively. These degradations increased to 0.8% and 0.5% after nearly 2.5 years [*Xiong et al*., 2002]. Recent studies of several Terra visible (VIS) and NIR bands show, however, a systematic wavelength-dependent drift of 2%–6% since 2003, and Terra-MODIS bands 1 and 2 suffered a drift of ~2% [*Wu et al*., 2013]. These all indicated the inadequacies in the MODIS SD/SDSM calibration system [*Wu et al*., 2013]. As a result, various improvements to the calibration algorithms have been adopted since launch. For example, MODIS calibration algorithms adopted a time-dependent response versus scan angle (RVS) since Collection 4 (C4), improved for Collection 5 (C5), and applied for the VIS bands for Collection 6 (C6), which is the latest version in operation. By using this version, *Doelling et al*. [2015] found the predicted Terra-MODIS bands 1 and 2 are now ~ +1%. In our study, both MODIS Collection 6 (MOD_C6) and Collection 4/5 SSF-MODIS (MOD_ssf) are used to examine the radiance calibration stability relative to the other two instruments, CERES and MISR.

MISR contains 36 parallel signal chains, corresponding to the four spectral bands in each of the nine cameras [*Diner et al*., 1998]. It uses an annual vicarious calibration to establish the radiometric response scale and a bimonthly OBC to track the radiometric stability [*Bruegge et al*., 2007]. For a bimonthly OBC over the poles, the panels are deployed to reflect diffuse sunlight into the standard detectors and the MISR CCD cameras simultaneously. The gain coefficients are then calculated for each of the 1504 photoactive pixels per line array and for each of the nine cameras and four spectral bands through linear regressions [*Chrien et al*., 2002; *Bruegge et al*., 2007].

It is believed that the MISR-OBC provides accurate camera-relative, band-relative, and pixel-to-pixel calibrations [*Abdou et al*., 2002]. Thanks to the blue-filtered high quantum efficiency photodiodes (HQE) that have remained stable to better than 0.5% for the first 2 years [*Chrien et al*., 2002], studies suggested the OBC-derived calibration coefficients successfully compensate for the steady approximately 2% year^{-1} decline of sensors' response over the mission [*Bruegge et al*., 2007]. More recent studies, however, showed that there

Table 1. Standard Criterion
$60° \le \theta_0 \le 70°$; Clear Percent $\ge 99.9\,\%$; homogeneous Indicator ≤ 0.02; and Near Nadir View and θ_v *B*etween Each Two Instruments $\le 5°$.

	Latitude	Longitude
Greenland Spot	74°N–76°N	39°W–42°W
Dome C	74°S–76°S	122°E–125°E

has been a drift of ~1.0% decade^{-1} in the nadir-view radiance for all spectral bands [*Bruegge et al.*, 2014], thought to be due to degradation of the HQE blue filter. Since MISR applies a forward processing strategy, the only current version (F03_0024) of radiance data set is used throughout this study.

3. Methodology

3.1. Study Region and Observations

Besides the OBC, sensors also applied intercalibration at specific targets to verify their radiometric calibration performances. Numerous studies have selected a variety of ground targets based on their purposes [*Teillet et al.*, 2007]. Among them, ice and snow fields, such as Greenland and Dome Concordia (Dome C), have been chosen due to their favorable surface and atmosphere conditions [*Loeb*, 1997; *Tahnk and Coakley*, 2001]. By using a 6 year data set over the Dome C, *Xiong et al.* [2009] found there was an approximately 1% relative calibration drift for bands 1 and 2 between two MODIS instruments in Collection 5. *Wu et al.* [2014] tracked the colocated MODIS and MISR reflectances and showed their red bands have a more scattered ratio trend than NIR bands. In general, ice and snow fields, especially Dome C, have attracted more and more attention as suitable sites for validation activities [*Xiong et al.*, 2009].

In this study we have also chosen Greenland Spot and Dome C (Table 1) as they offer many advantages. Both are stable regions with permanent snow cover and are viewed frequently by a polar orbiter. They are far enough from each other to provide independent samples. They also have distinct atmospheric precipitable water contents (PWC). The PWC of Dome C is far less than that of Greenland Spot, where relatively bigger annual variation is found. This can help us to understand the role of water vapor in the relationship between broadband and spectral band radiances.

Wu et al. [2014] found the blue band of MODIS could saturate over Dome C. As a result we did not include the blue band in this study. In addition, the green band was also excluded due to the absence of MODIS green band radiances in the CERES SSF data set.

Overall, in this study, three kinds of data set from CERES, MODIS, and MISR over two polar regions have been used to investigate the intercalibration differences. The study period includes 15 April months for Greenland Spot and 15 October months for Dome C, from 2001 to 2015. CERES shortwave broadband radiances come from SSF Terra-FM1 Ed3A. MISR spectral band radiances come from MISR_AM1_GRP_ELLIPSOID_AN_F03_0024. For MODIS radiances, one data set is MOD021KM Collection 6 (MOD_C6) and the other is contained in the CERES SSF data set (MOD_ssf).

3.2. Radiance Colocation

Since all three instruments are on the same Terra spacecraft, their measurements can be colocated. Due to the different observation configurations, the two spectroradiometers, MODIS and MISR, can be well matched. But not all of their scenes can be assigned to a corresponding CERES field of view (FOV). This is because CERES is a scanner with a typical 6.6 s cross-track scan cycle [*Wielicki et al.*, 1996]. Thus, in this study, near-nadir observations from CERES (20 km nadir resolution) were treated as the standard scenes, and all MODIS (1 km nadir resolution) near-nadir radiances from the same orbit were assigned to a CERES scene if they satisfied the criterion, $d \le 10$ km, where

$$d = \sqrt{111 \cdot (\mathrm{lat}_{\mathrm{CERES}} - \mathrm{lat}_{\mathrm{MODIS}})^2 + \left(111 \cdot \cos\left(\frac{\mathrm{lat}_{\mathrm{CERES}} + \mathrm{lat}_{\mathrm{MODIS}}}{2}\right) \cdot (\mathrm{lon}_{\mathrm{CERES}} - \mathrm{lon}_{\mathrm{MODIS}})\right)^2} \quad (1)$$

and $\mathrm{lat}_{\mathrm{CERES}}$ and $\mathrm{lon}_{\mathrm{CERES}}$ ($\mathrm{lat}_{\mathrm{MODIS}}$ and $\mathrm{lon}_{\mathrm{MODIS}}$) represent the latitude and longitude of a CERES (MODIS) near-nadir FOV. *d* is thus the distance between the centers of the two instruments' FOV. The quality of radiance colocation can be controlled by setting the maximum allowance of *d*. We chose $d \le 10$ km in this study since the radius of CERES nadir footprint is ≈ 10 km, ensuring all MODIS FOV are at least 50% within the CERES

FOV. The corresponding MODIS mean radiance for a CERES scene is then calculated by averaging all the valid MODIS observations. Perfect integration over the CERES footprint is not essential due to the choice of homogeneous target regions. For every CERES point with a valid MODIS value, a MtkRegion R with CERES center latitude, longitude, and expanded by 10 km was set by MisrToolkit (equation (2)), provided by the Jet Propulsion Laboratory. The toolkit then provided the corresponding MISR mean radiance as well as the standard deviation of these subpixel red band radiances, which is used as a homogeneity indicator in this study. Further details on the MisrToolkit can be found on the MISR website https://eosweb.larc.nasa.gov/project/misr/tools/misr_toolkit.

$$R = \mathrm{MtkRegion}(\mathrm{lat_{CERES}}, \mathrm{lon_{CERES}}, 10.0, 10.0, \text{″km″}) \tag{2}$$

3.3. Normalized Radiance Ratio

In this study, the red and NIR spectral bands from both MODIS and MISR, and one shortwave broadband (BB) from CERES are used. We did not separate the MODIS measurements by their detector and mirror side because we are focusing on the instrument itself. Although the degradation of each MODIS spectral band is both detector and mirror-side dependent, mean band degradation can be achieved by taking into account a large number of MODIS measurements.

For any given orbit, or day, and sensor pairs A and B, we obtain a mean daily ratio of radiances $r_i = \langle I_A/I_B \rangle$ where I_A or I_B may be in units of $\mathrm{W\,m^{-2}\,sr^{-1}\,\mu m^{-1}}$ or $\mathrm{W\,m^{2}\,sr^{-1}}$, depending on whether the sensor is spectral or broadband. Monthly mean radiance ratios, R_G(year) and R_D(year), are determined by taking average of r_i for all available days in April for Greenland and in October for Dome C, respectively. The corresponding error bars σ_{year} in the following analysis were one standard deviation of the r_i for the same temporal and spatial range. Finally, taking 2001 as the reference, we work with normalized ratios, $\Delta R(\mathrm{year}) = \dfrac{R(\mathrm{year}) - R(2001)}{R(2001)}$.

We applied a weighted least squares (WLS) method for the trend analysis by taking into account the 15 normalized ratios and their corresponding error bars (1σ). If the two instruments are relatively stable with respect to each other, their normalized ratios should show no trend over the years. However, if there is a significant trend in the normalized ratios that is consistent for the two regions, it is reasonable to expect the trend is due to an intercalibration difference.

4. Results

By using the normalized radiance ratios from CERES, MODIS, and MISR, intercalibration differences can be examined. In this study, Greenland Spot and Dome C are analyzed separately, containing comparisons between CERES/MISR, CERES/MOD_C6(ssf), and MOD_C6(ssf)/MISR radiance ratios. The standard criteria in stratifying the colocated data set are shown in Table 1.

4.1. Radiance Field

By applying these criteria (Table 1) to the data, Figure 1 shows the monthly mean (April for Greenland and October for Dome C) radiances as well as their anomalies, which were the radiances normalized with their corresponding value of 2001. It is clear that Dome C (Figure 1b) is far more stable than the Greenland Spot (Figure 1a). This is expected since Dome C is one of the most stable areas on Earth. The NIR and BB radiances show similar variability, in both pattern and magnitude. The red radiances vary with a similar pattern, but with greater amplitude, indicating greater sensitivity to variations in the surface or atmosphere, such as water vapor and ozone amount. Since red radiances are much larger than BB or NIR radiances, it is hard to draw conclusions directly from the radiance trends within the two regions.

The well-matched relative anomalies in both regions suggest the validity of our radiance colocation method. They also indicate perceptible increasing trends, especially for the MOD_C6 Red band in Dome C. In order to further investigate these signals, normalized ratios (ΔR) are used in the following sections.

4.2. Relationship Between PWC and Broad:Spectral Radiance Ratio

Atmospheric effects on broadband solar radiation, especially due to O_3 and H_2O, have been well known for a long time [*Paltridge and Platt*, 1976]. Yet controversial results have been shown in the narrow-to-broadband radiance conversion. *Li et al*. [1999] found the effect of O_3 was minimal while H_2O had up to 5% effect on the

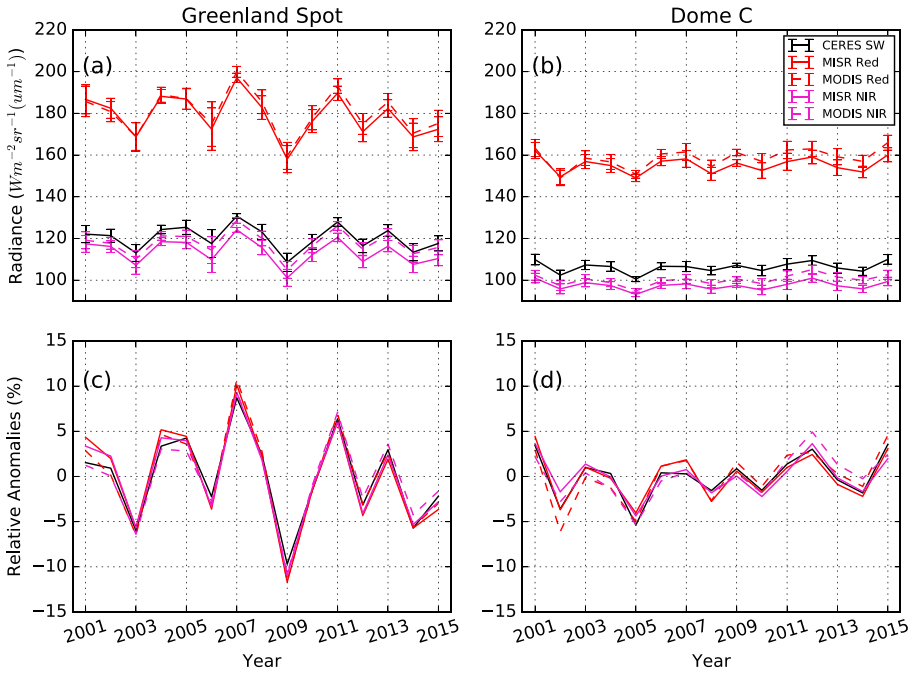

Figure 1. Direct colocated radiances (W m^{-2}sr^{-1} or W m^{-2}sr^{-1} μm^{-1}) and corresponding anomalies (%) for (a, c) April Greenland Spot and (b, d) October Dome C.

conversion. This was supported by *Buriez et al.* [2007] who found an increased explained variance of their regression from 0.990 to 0.994, after taking into account H_2O and O_3 correction terms. *Loeb et al.* [2006], however, suggested there was no evident improvement after binning data by precipitable water (H_2O) in a small range. In order to investigate the role of low water vapor content in the relationship between spectral and broadband radiances, six years (2001–2007) of October CERES SW and MOD_ssf data were analyzed. The selected data came from the eastern part of the Antarctica (75°S ~ 85°S, 0° ~ 180°E) within a small angular

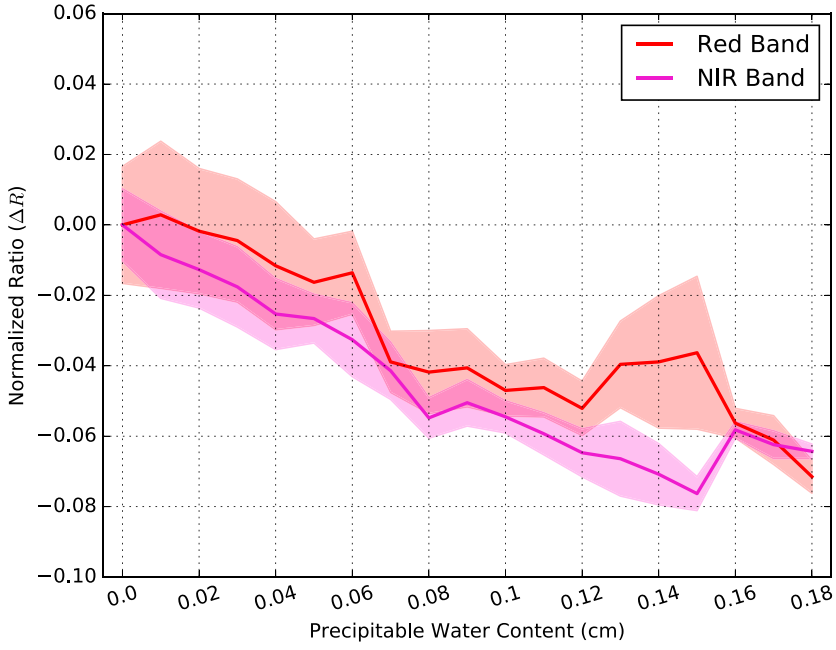

Figure 2. Relationship between Precipitable Water Content (PWC) and CERES:MOD_ssf red and NIR radiance ratio. The ratios have been normalized to the PWC∈ [0.0,0.01) case, and the colored areas represent the range of uncertainties.

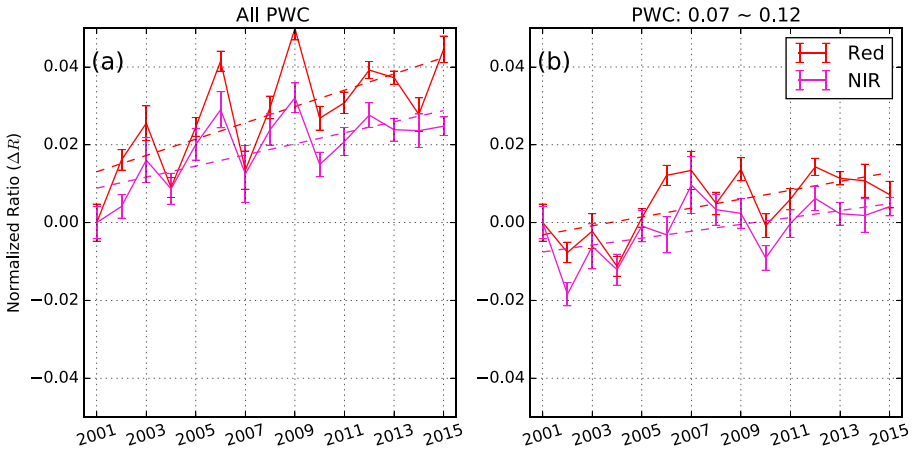

Figure 3. Normalized ratios of CERES SW and MISR red and NIR bands over Greenland Spot (a) before and (b) after applying PWC criterion.

range ($70° \leq \theta_0 \leq 72°$, $\theta_{v_{CER}} \leq 10°$, and $|\theta_{v_{CER}} - \theta_{v_{MOD}}| < 5°$). The reason for choosing this shorter period is that since 2007 the MODIS data contained in the SSF data set suffered a serious drop [*Wu et al.*, 2013], which will also be discussed below.

Figure 2 shows the dependence of the CERES:MOD_ssf red and NIR radiance ratios retrieved from SSF data set on precipitable water content (PWC). The shaded areas around the central lines are one standard deviation of ratios within the corresponding PWC range. It is clear that there is a strong negative dependence of the normalized ratio on PWC for both bands. This result is expected because of water vapor absorption outside the red and NIR bands.

The NIR band appears to have a greater dependence on PWC, with less variability, than that the red band, for PWC < 0.15 cm. The red band may be influenced by additional factors (e.g., snow thickness change caused by the permanent snow melting) that complicate its dependence on PWC.

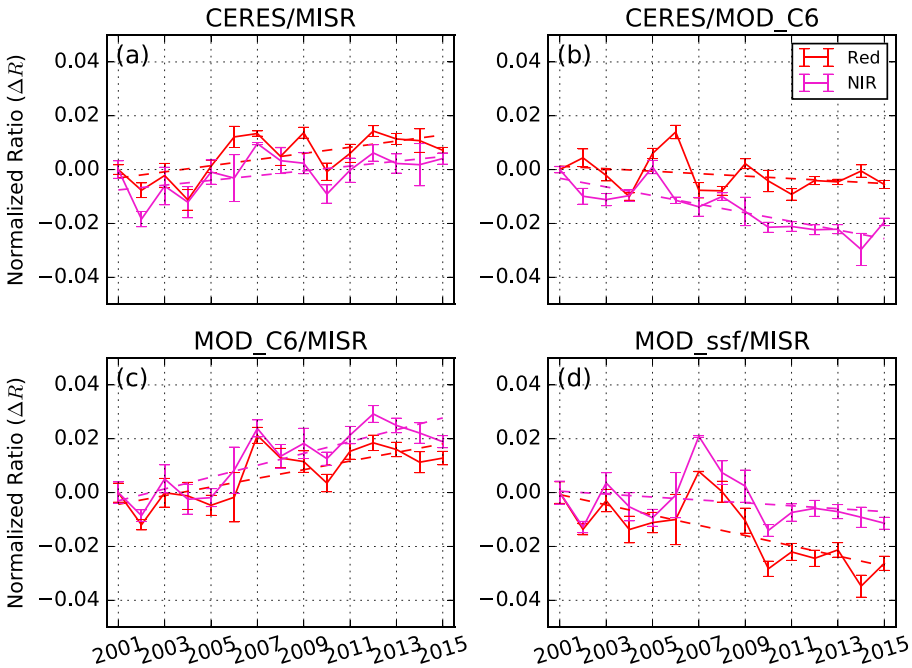

Figure 4. Greenland Spot case of normalized radiance ratio trends for successive Aprils, for (a) CERES against MISR, (b) CERES against MODIS Collection 6, (c) MODIS Collection 6 against MISR, and (d) MODIS SSF against MISR. Data were limited to $0.07 \leq \text{PWC} \leq 0.12$ cm.

Table 2. Statistics Results for Interinstrument Calibration Differences Among CERES Ed3A, MISR, and MODIS Collection 6

WLS Fitting Slope ± Standard Error		CERES-MISR	CERES-MODIS	MODIS-MISR
Greenland Spot	Red	0.011 ± 0.004	− 0.004 ± 0.003	0.017 ± 0.004
	NIR	0.009 ± 0.004	− 0.015 ± 0.003	0.023 ± 0.004
Dome C	Red	0.009 ± 0.004	− 0.016 ± 0.006	0.024 ± 0.003
	NIR	0.012 ± 0.005	− 0.013 ± 0.006	0.023 ± 0.003

To investigate the influence of PWC on the broad:spectral radiance ratio trends, Figure 3 shows a comparison of the CERES:MISR radiance ratios before and after binning by the PWC. Although further binning the data set reduced available colocated FOVs, causing relative larger variances in some years, it significantly affected the ratio trends. The trends of CERES:MISR radiance ratio decreased from 2.4 ± 0.7% decade^{-1} to 1.6 ± 0.4% decade^{-1} for the MISR red band, and from 1.7 ± 0.5% decade^{-1} to 1.2 ± 0.4% decade^{-1} for the NIR band, indicating a strong influence of PWC on the broad:spectral radiance ratios. In order to minimize the bias that could be caused by the water vapor, two small PWC intervals are chosen for Greenland ($0.07 \le PWC \le 0.12$ cm) and Dome C ($0.01 \le PWC \le 0.02$ cm). They are different because Dome C is much drier than Greenland.

4.3. Radiance Stability

By taking into account PWC, normalized ratios are calculated from colocated CERES, MODIS, and MISR near-nadir radiances. Five instrument pairs are compared over both Greenland Spot and Dome C to examine whether their radiances are stable relative to one another during the past 15 years. The comparisons are restricted to CERES FM1 cross-track SW radiances, MODIS radiances in the 0.65 μm (red) and 0.86 μm (NIR) bands from both the CERES SSF and MODIS Collection 6 product, and MISR ELLIPSOID 0.67 μm (red) and 0.86 μm (NIR) bands radiances. Figure 4 shows the year-to-year mean radiance ratios within the Greenland Spot. The corresponding WLS fitting slopes and standard errors are listed in Table 2. The comparison between CERES and MOD_ssf is not shown in the figure as the space is limited. All the ratios have been normalized to the values of 2001, allowing us to track the calibration difference between each two-sensor pair since then.

Results indicate that the calibration differences among the three instruments are up to 2.4% decade^{-1} during the study period. Specifically, for both spectral bands, CERES is getting brighter compared with MISR and darker compared to MOD_C6. Although MISR shows significant darkening trends compared to MOD_C6, it barely changed compared to MOD_ssf, especially for 2001–2006. It should be noted that MOD_ssf changed

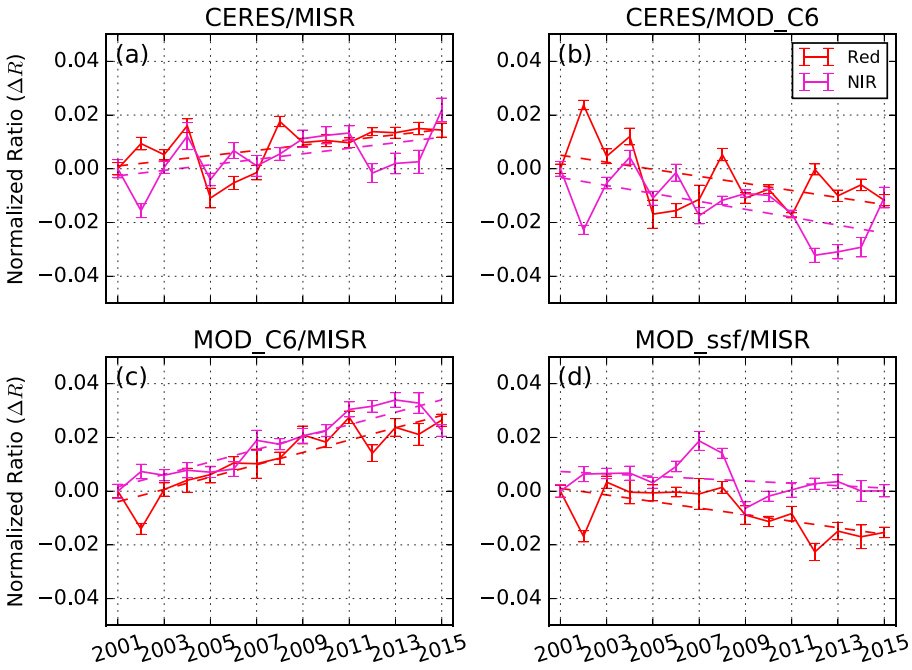

Figure 5. Same as Figure 4 but for successive Octobers in Dome C. Data were limited to $0.01 \le PWC \le 0.02$ cm.

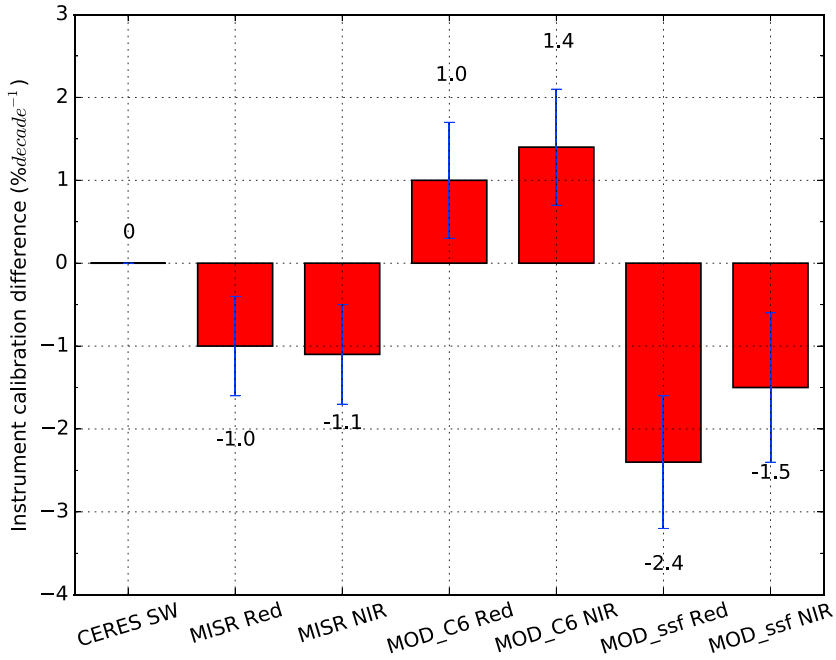

Figure 6. Instrumental calibration differences (% decade^{-1}) relative to the CERES SW broadband.

to the MODIS Collection 5 since 2007, indicating MISR could have remained stable relative to the MODIS Collection 4.

Consistent results can be found in Dome C (Figure 5), where October data are considered. Compared to the Greenland Spot, the normalized ratios are more consistent over the Dome C for both spectral bands. This is expected since Dome C is more stable in atmospheric and surface conditions than Greenland Spot. The precipitable water content has also remained quite low throughout the 15 Octobers. Furthermore, while the trends over the two regions are all consistent within their uncertainties, spectral:spectral radiance ratios show the strongest consistency (Figures 4c and 5c). Specifically, for the red band, MISR shows darkening trends compared to MODIS Collection 6, at −1.7% decade^{-1} and −2.4% decade^{-1} for Greenland Spot and Dome C, respectively. These two values become identical (−2.3% decade^{-1}) for their NIR bands. The larger bias in the red band is believed to be caused by the relatively larger mismatch in their red wavelengths.

We do not show results from unrestricted PWC as Greenland Spot showed much larger changes than Dome C, with greater variability in the red band, consistent with Figure 2. This is due to the greater range of conditions apparent for Greenland Spot.

Overall, since the two study regions are far from each other, their consistency indicates the existence of intercalibration differences among the CERES, MODIS, and MISR. For their current radiance products, there is a calibration difference of ~2.0% decade^{-1} between MISR ELLIPSOID data set and MODIS Collection 6 data set. CERES, on the other hand, is brightening at ~1.0% decade^{-1} compared to MISR and darkening at ~ −1.0% decade^{-1} relative to MODIS Collection 6.

Table 3. Same as Table 2 But for MOD_ssf Data Set

WLS Fitting Slope ± Standard Error		CERES-MODIS	MODIS-MISR
Greenland Spot	Red	0.032 ± 0.004	− 0.030 ± 0.01
	NIR	0.015 ± 0.006	− 0.010 ± 0.01
Dome C	Red	0.015 ± 0.007	− 0.011 ± 0.004
	NIR	0.015 ± 0.007	− 0.004 ± 0.004

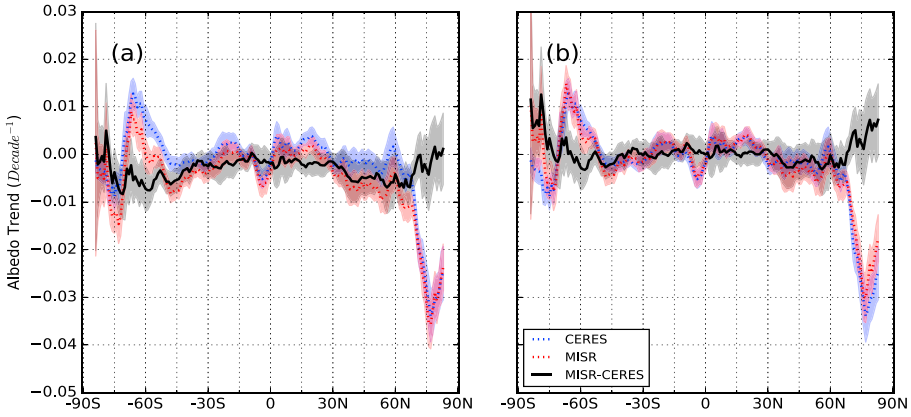

Figure 7. Latitudinal decadal trend of TOA albedo, (a) before and (b) after applying a correction coefficient of +1% decade^{-1} for CERES-MISR intercalibration.

5. Application

A summary of the intercalibration differences of all bands relative to the CERES SW is shown in Figure 6. More detailed results can be found in Tables 2 and 3. It is clear that the calibration differences between the current version of CERES and MODIS (MISR) are within ±2% decade^{-1} since 2001. MISR shows a darkening trend of ~ −1.0% decade^{-1} compared to CERES SW broadband, while MODIS indicates a brightening trend of ~1.0% decade^{-1} compared to CERES SW broadband. Moreover, our results are consistent with the conclusions from independent studies. Specifically, Bruegge (personal communication, 2016) found that MISR has likely suffered an uncorrected calibration drift of −1.0% decade^{-1}. *Doelling et al*. [2015] suggested that Terra-MODIS for bands 1 and 2 are ~1.0% decade^{-1} in its Collection 6. Recently, *Daniels et al*. [2015] claimed that CERES FM1 SW channel only has an insignificant trend of 0.15% decade^{-1}. Based on the aforementioned results, it appears that CERES has remained more stable than MODIS and MISR. In addition, these intercalibration differences can be used as correction coefficients to investigate the long-term trends of high-level products of those instruments, such as the top-of-atmosphere (TOA) albedo.

Figure 7 shows the latitudinal decadal trends of TOA albedo from the CERES and MISR monthly TOA albedo products, SSF1deg-lite-Month Terra Ed2.6 and MISR Level 3 Component Global Albedo products. The corresponding shortwave flux trends can be seen in Figure 8. Both trend and uncertainty (shown as the colored area) are calculated for each 1.0° latitude. It is clear that the two data sets exhibit similar trends at all latitudes, and the decadal trend differences are within ±0.01 for TOA albedo and ±2 W m^{-2} for SW flux. However, MISR captures a notable darkening across the Northern Hemisphere's midlatitudes that is not shown by CERES.

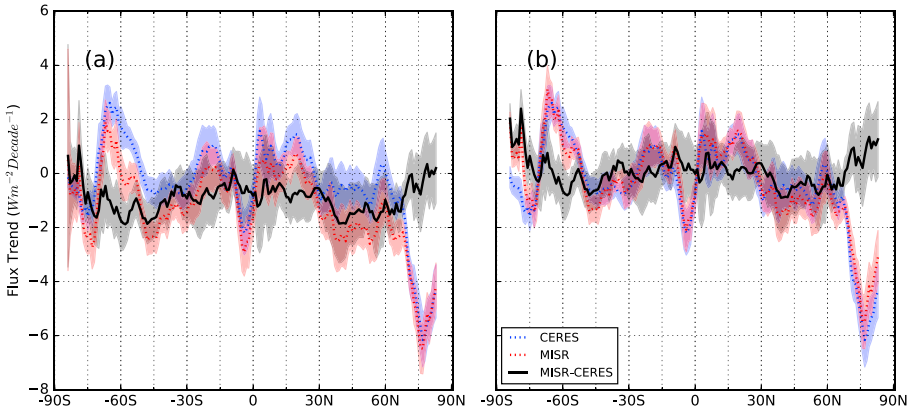

Figure 8. Same as Figure 7 but for TOA flux.

Globally, MISR indicates a darkening Earth with $-1\,W\,m^{-2}\,decade^{-1}$, while CERES suggests an unchanged Earth. It is also noted that the latitudinal flux trends show more oscillation than the albedo trends, a consequence of latitude-dependent insolation.

Since the MISR SW albedos come from scene-dependent combinations of its spectral albedos, we applied a correction coefficient (+1% $decade^{-1}$) to its broadband albedo product to account for their intercalibration difference. The results are encouraging after correction (Figures 7b and 8b). The two data sets correspond very well except at the high latitudes, where the largest differences of instantaneous TOA albedo were found (not shown). Globally, MISR shows an unchanged Earth just like CERES. The positive bias of TOA albedo at high latitudes is likely caused by the different albedo retrieval methods adopted by the two instruments. As an example, CERES and MISR apply different approaches to identify snow/ice scenes. This may affect their choice of anisotropic reflection model. While CERES adopts a daily snow/ice mask, MISR currently uses a monthly snow/ice mask, which labels a $1°\times1°$ region as snow/ice if four or more days out of the month had snow or ice present. Thus, MISR may overestimate the snow/ice area in the summer months when the sea ice extent changes rapidly, leading to the less significant darkening in the polar regions. Further studies are needed to quantify the differential albedo trends shown by CERES and MISR over the polar regions.

6. Discussion and Conclusions

In this study, coincident CERES, MODIS, and MISR near-nadir radiances are collected for two regions (Greenland Spot and Dome C) to investigate the intercalibration differences among the three sensors. The choice of these regions worked well, with Dome C being the superior site, corroborated by Greenland Spot. The radiance data of the three instruments are from their current releases, SSF FM1 Edition 3A for CERES, Collection 6 for MODIS, and F03_0024 for MISR. Since SSF also includes the previous collections of MODIS radiances, they were also analyzed to show the difference between MODIS collections. Seven years of October CERES SSF data over Eastern Antarctica were also used to determine whether the precipitable water content affects the broad-spectral radiance ratio even for very dry atmospheric conditions. Our results show a strong negative correlation between the radiance ratio and PWC in both red and near-infrared bands, indicating that water vapor needs be taken into account in the broad-spectral radiance relationship, even for dry conditions. Moreover, the red band has a more complicated dependence than the near-infrared band, indicated by the larger uncertainty range in Figure 2. This may explain the more variable ratio trends between broadband and red band.

After further binning the colocated radiance ratios by a narrow range of PWC, trends of the calibration differences were calculated by the WLS method, which uses normalized mean radiance ratios as regression points and inversed variance of the ratios as weights. Although Dome C and Greenland show consistent results, because of a more stable surface and atmospheric (water vapor content) conditions, Dome C could be a better target for instruments' intercalibration, especially for broadband and spectral-band comparison. However, Greenland is also feasible once additional information is used to bin the data. Regarding the two spectroradiometers, there are significant radiance ratio trends in the current collections of MISR and MODIS. A calibration difference up to 2.4% $decade^{-1}$ is found between their red radiances, in agreement with *Wu et al*. [2014]. Interestingly, as shown by *Loeb et al*. [2007] and here, MODIS radiances included in the CERES SSF product do not show such trends, especially in the near-infrared band. This suggests the latest update (Collection 6) of MODIS calibration coefficients is responsible for the radiance drift. Regarding CERES and MISR, results show statistically consistent trends in both red and near-infrared bands, ~1.0% $decade^{-1}$. This small but systematic trend is larger than the Earth Radiation Budget requirement of 0.3% $decade^{-1}$, as indicated by *Ohring et al*. [2005]. As a result, this needs to be taken into account before doing the trend comparison of their high-level products. By considering their shortwave TOA albedo products, we show that the latitudinal trends inferred from the two data sets correspond very well after correction, except for the high latitudes. This confirms the finding of *Sun et al*. [2006] that consistent TOA albedos can be obtained by the two instruments over low-latitude and midlatitude regions. It also suggests more effort should be put into comparing their TOA albedos over the polar regions. Because there is no "standard" instrument, we cannot tell which one is better than the other. However, CERES calibration may be referenced as a proxy for "truth," based on results from this paper and previous studies [*Bruegge et al*., 2014; *Daniels et al*., 2015; *Doelling et al*., 2015]. In this scenario, an unchanged global average and midnorthern latitudes TOA albedo, based on CERES, are achieved.

Overall, thanks to their own onboard calibration systems, CERES, MODIS, and MISR have each been successfully operated for more than 15 years with independent calibration. Intercalibration shows that compared to CERES SW, the current versions of MISR and MODIS show calibration differences of approximately −1% decade^{-1} and +1.2% decade^{-1}, respectively, consistently for two independent target areas. These intercalibration differences provide a degree of synergy that is reassuring and that can also be used to fine tune systematic discrepancies between their high-level products.

Acknowledgments

We thank D.J. Diner and C.J. Bruegge for helpful discussions. This work was supported by Subcontract 1460339 between the California Institute of Technology/Jet Propulsion Laboratory and the University of Auckland. The original CERES SSF and MISR L1B2E data sets were obtained from the NASA Langley Research Center Atmospheric Science Data Center, https://eosweb.larc.nasa.gov/. The MODIS data sets were obtained from the NASA Level 1 and Atmosphere Archive and Distribution System (LAADS), https://earthdata.nasa.gov/about/daacs/daac-laads. All other numerical information is provided in the figures and tables produced by solving the equations in the paper.

References

Abdou, W. A., C. J. Bruegge, M. C. Helmlinger, J. E. Conel, S. H. Pilorz, W. Ledeboer, B. J. Gaitley, and K. J. Thome (2002), Vicarious calibration experiment in support of the multi-angle imaging spectroradiometer, *IEEE Trans. Geosci. Remote Sens.*, *40*(7), 1500–1511, doi:10.1109/TGRS.2002.801582.

Bruegge, C. J., D. J. Diner, R. A. Kahn, N. Chrien, M. C. Helmlinger, B. J. Gaitley, and W. A. Abdou (2007), The MISR radiometric calibration process, *Remote Sens. Environ.*, *107*(1–2), 2–11, doi:10.1016/j.rse.2006.07.024.

Bruegge, C. J., S. Val, D. J. Diner, V. Jovanovic, E. Gray, L. DiGirolamo, and G. Zhao (2014), Radiometric stability of the Multi-angle Imaging SpectroRadiometer (MISR) following 15 years on-orbit, *Proc. SPIE*, *9218*, 1–11, doi:10.1117/12.2062319.

Buriez, J.-C., F. Parol, Z. Poussi, and M. Viollier (2007), An improved derivation of the top-of-atmosphere albedo from POLDER/ADEOS-2: 2. Broadband albedo, *J. Geophys. Res.*, *112*, D19201, doi:10.1029/2006JD008257.

Chrien, N. L., C. J. Bruegge, and R. R. Ando (2002), Multi-angle Imaging SpectroRadiometer (MISR) On-Board Calibrator (OBC) in-flight performance studies, *IEEE Trans. Geosci. Remote Sens.*, *40*(7), 1493–1499.

Daniels, J. L., G. L. Smith, K. J. Priestley, and S. Thomas (2015), Using lunar observations to validate in-flight calibrations of clouds and the Earth's Radiant Energy System instruments, *IEEE Trans. Geosci. Remote Sens.*, *53*(9), 5110–5116, doi:10.1109/TGRS.2015.2417314.

Diner, D. J., et al. (1998), Multi-angle Imaging SpectroRadiometer (MISR) instrument description and experiment overview, *IEEE Trans. Geosci. Remote Sens.*, *36*(4), 1072–1087, doi:10.1109/36.700992.

Doelling, D. R., A. Wu, X. Xiong, B. R. Scarino, R. Bhatt, C. O. Haney, D. Morstad, and A. Gopalan (2015), The radiometric stability and scaling of collection 6 Terra- and Aqua-MODIS VIS, NIR, and SWIR spectral bands, *IEEE Trans. Geosci. Remote Sens.*, *53*(8), 4520–4535, doi:10.1109/TGRS.2015.2400928.

Guenther, B., X. Xiong, V. V. Salomonson, W. L. Barnes, and J. Young (2002), On-orbit performance of the Earth Observing System Moderate Resolution Imaging Spectroradiometer; first year of data, *Remote Sens. Environ.*, *83*, 16–30, doi:10.1016/S0034-4257(02)00097-4.

Lee, R. B., B. R. Barkstrom, G. L. Smith, J. E. Cooper, L. P. Kopia, and R. W. Lawrence (1996), The Clouds and the Earth's Radiant Energy System (CERES) sensors and preflight calibration plans, *J. Atmos. Oceanic Technol.*, *13*, 300–313.

Li, Z., A. P. Trishchenko, H. W. Barker, G. L. Stephens, and P. Partain (1999), Analyses of Atmospheric Radiation Measurement (ARM) program's Enhanced Shortwave Experiment (ARESE) multiple data sets for studying cloud absorption, *J. Geophys. Res.*, *104*(D16), 19,127–19,134, doi:10.1029/1999JD900308.

Loeb, N. G. (1997), In-flight calibration of NOAA AVHRR visible and near-IR bands over Greenland and Antarctica, *Int. J. Remote Sens.*, *18*(3), 477–490, doi:10.1080/014311697218908.

Loeb, N. G., W. Sun, W. F. Miller, K. Loukachine, and R. Davies (2006), Fusion of CERES, MISR, and MODIS measurements for top-of atmosphere radiative flux validation, *J. Geophys. Res.*, *111*, D18209, doi:10.1029/2006JD007146.

Loeb, N. G., B. A. Wielicki, W. Su, K. Loukachine, W. Sun, T. Wong, K. J. Priestley, G. Matthews, W. F. Miller, and R. Davies (2007), Multi-instrument comparison of top-of-atmosphere reflected solar radiation, *J. Clim.*, *20*(3), 575–591, doi:10.1175/JCLI4018.1.

Matthews, G., K. Priestley, P. Spence, D. Cooper, and D. Walikainen (2005), Compensation for spectral darkening of short wave optics occurring on the cloud's and the Earth's radiant energy system, *Proc. SPIE*, *5882*, 1–12, doi:10.1117/12.618972.

Ohring, G., B. Wielicki, R. Spencer, B. Emery, and R. Datla (2005), Satellite instrument calibration for measuring global climate change: Report of a workshop, *Bull. Am. Meteorol. Soc.*, *86*(9), 1303–1313, doi:10.1175/BAMS-86-9-1303.

Paltridge, G. W., and C. M. R. Platt (1976), *Radiative Processes in Meteorology and Climatology*, Elsevier Scientific, New York.

Sun, J., A. Angal, X. Xiong, H. Chen, X. Geng, A. Wu, T. Choi, and M. Chu (2012), MODIS reflective solar bands calibration improvements in Collection 6, *Proc. SPIE*, *8528*, 1–10, doi:10.1117/12.979733.

Sun, W., N. G. Loeb, R. Davies, K. Loukachine, and W. F. Miller (2006), Comparison of MISR and CERES top-of-atmosphere albedo, *Geophys. Res. Lett.*, *33*, L23810, doi:10.1029/2006GL027958.

Tahnk, W. R., and J. A. Coakley (2001), Updated calibration coefficients for NOAA-14 AVHRR Channels 1 and 2, *Int. J. Remote Sens.*, *22*(15), 3053–3057, doi:10.1080/01431160120423.

Teillet, P. M., J. A. Barsi, G. Chander, and K. J. Thome (2007), Prime candidate Earth targets for the post-launch radiometric calibration of space-based optical imaging instruments, *Proc. SPIE*, *6677*, 1–12, doi:10.1117/12.733156.

Weatherhead, E. C., et al. (1998), Factors affecting the detection of trends: Statistical considerations and applications to environmental data, *J. Geophys. Res.*, *103*(D14), 17,149–17,161, doi:10.1029/98JD00995.

Wielicki, B. A., B. R. Barkstrom, E. F. Harrison, R. B. Lee, G. L. Smith, and J. E. Cooper (1996), Clouds and the Earth's Radiant Energy System (CERES): An Earth Observing System Experiment, *Bull. Am. Meteorol. Soc.*, *77*, 853–868, doi:10.1175/1520-0477(1996)077<0853:CATERE>2.0.CO;2.

Wu, A., X. Xiong, D. R. Doelling, D. Morstad, A. Angal, and R. Bhatt (2013), Characterization of Terra and Aqua MODIS VIS, NIR, and SWIR spectral bands' calibration stability, *IEEE Trans. Geosci. Remote Sens.*, *51*(7), 4330–4338.

Wu, A., A. Angal, and X. Xiong (2014), Comparison of coincident MODIS and MISR reflectances over the 15-year period of EOS Terra, *Proc. SPIE*, *9218*, 1–13, doi:10.1117/12.2061117.

Xiong, X., A. Wu, and B. N. Wenny (2009), Using Dome C for moderate resolution imaging spectroradiometer calibration stability and consistency, *J. Appl. Remote Sens.*, *3*(1), 1–12, doi:10.1117/1.3116663.

Xiong, X. J., A. Wu, J. A. Esposito, J. Sun, N. Che, B. Guenther, and W. L. Barnes (2002), Trending results of MODIS optics on-orbit degradation, *Proc. SPIE*, *4814*, 337–346.